

Optimal Inversion of Array Induction Log

Dongliang Liao

(Well Logging Technology Department, SINOPEC Research of Petroleum Engineering, Beijing 100101, China)

ABSTRACT Multi-array induction logging is one of the most important imaging logs and plays significant roles on evaluation of complicated reservoirs. It simultaneously measures multiple induction logs in different invasion depths through an arraying coil system, and obtains a radial resistivity profile after inversion. The inversion process depends on both the design of formation model and the selection of proper algorithm. According to the geometry factor theory, respond functions and features can be constructed and characterized. This paper applies the optimized method to inverse three resistivity's zones (for flushed zone, transitional zone and undisturbed zone respectively) and two radial depths (flushed depth and invaded depth) with different formation resistivity models (i.e. step-invaded model, exponent-invaded model, reciprocal-invaded and parabolic-invaded model). The fast inversion algorithm based on BFGS(a algorithm proposed by four authors: Broyden, Fletcher, Goldfarb and Shanna) and PIA(parabola interpolation algorithm) is suitable for long section processing and has been demonstrated well by three applications. The optimal method in this paper can be applied in inverting formation resistivity, invade depth and identifying low resistivity annulus zone. According to the inversion results, industrial oil flow has been found successfully.

KEY WORDS: array induction; optimal method; resistivity curves; inversion; resistivity model; proper algorithm

Date of Submission: 13-10-2020

Date of Acceptance: 29-10-2020

I. INTRODUCTION

The sub-array signals are collected by array induction log, after synthesizing and matching the resolution, the matched data is directly used in the inversion. However, this method is time-wasting and complicated, it is only applied to permeable formation in most cases which restricts its application^[1-10]. This paper introduces a geometry factor analysis method and formation resistivity models, constructs the log response equation, chooses the optimum algorithm to inverse the data by adjusting the models and computes the deviation between the forward modeling results and practical logging curves. The effect of the inversion depends on the design of the models and the algorithm, it can be discriminated in accordance with the confidence intervals and values of objective function.

In previous work, Lin et al.(1984) chose the least square algorithm to obtain the formation parameters with induction logging^[1], however, this method was too simple to deal with complicated formation profile.; Chew et al.(1994) used the distorted Born iterative method and CG-FFHT to inverse the induction logs^[2], unfortunately, this way imaged two-dimension resistivity profile with a less accuracy; Zhang Z Q et al.(1997) applied the quasi linear approximation theory to reverse array induction synthetic matrix, consequently introduced the multi inversion with Marquardt and SAM-FFHT algorithm^[3-4], in the paper Zhang Z Q proposed the conception of pixel, which improved inversion accuracy, obtaining a resistivity profile, but this method could not receive a reasonable inversion result when formation has a low or high resistivity annulus zone. Zhang Y R et al.(1997) adopted the non-linear integral method^[5], this algorithm is based on precise iterative method of nonlinear integral equations, obtaining formation resistivity profile by using regularization method, it also has a disadvantage that the effect of abnormal conductivity in invaded zone is inevitable. While Wei B J et al. (2005) employed the integral equations^[6].

Previous researchers are able to invert the array induction, but when the formation has low or high resistivity, unreasonable result can be worked out. This paper analyses one dimension and multi-dimension searching algorithms according to the objective functions features by using a stable and highly efficient algorithm. In terms of inversion models, linear variation model and reciprocal model are commonly employed^[7-9] in the transitional zone, which is unable to produce a certain inversion result between transition zones resistivity and logging resistivity values, especially encounters low or high resistivity annulus zones. Thus, the optimal model is selected by comparing different inversion results of the following four models in this paper. The optimal method in this paper can be applied in inverting formation resistivity, invade depth and identifying low resistivity annulus zone. According to the inversion results, industrial oil flow has been found successfully.

II. COIL SYSTEM IN ARRAY INDUCTION LOG

2.1 Coil system Structure

The coil system of array induction tool consists of one dominant transmitter coil and several receiver coils. Each of the receiver coil system includes one dominant receiver coil and one dominant shielded coil, making up a three-coil system sub-array with the main transmitter coil.

In Fig.1, AIT instrument has eight asymmetric sub-arrays with three types of working frequencies, which can draw five curves of different depth of investigation through software synthetic focusing; HDIL instrument contains seven unilateral sub-array and eight working frequencies, it can produce six curves of different depth of investigation through the software synthetic focusing; the arrangement of HRAI instrument is quite different, which places the dominant transmitter coil right in the middle, five receiver coils in ups and downs respectively, the sub-arrays are asymmetric except the shortest one. HRIA has two working frequencies and generates six curves of different depth of investigation after the software synthetic focusing.

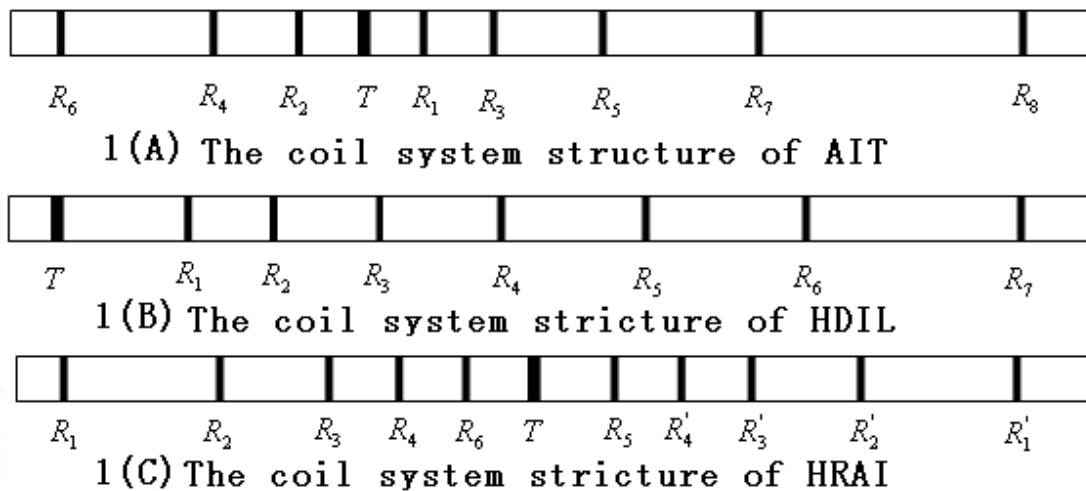


Fig.1 Sketch map of coil system in different array induction tools

2.2 Geometry factor of array induction tools

For the array induction logging, the geometry factors are used to describe the contribution of each component to the measured signal. The relationship between the measured signal σ_a and formation signal σ is

$$\sigma_a(z) = \int_0^{\infty} \int_{-\infty}^{\infty} g_{Doll}(\rho', z - z') \sigma(\rho', z') d\rho' dz' \quad (1)$$

Where, $g_{Doll}(\rho, z) = \frac{L}{2} \left(\frac{\rho}{r_T r_R} \right)^3$ is the Doll geometry factor, r_T and r_R are the distance from the point

$P(\rho, z)$ to the transmitter coil and the receiver coil in cylindrical coordinates respectively, L is the distance between the transmitter and the receiver coil^[11].

The radial geometry factor predicts the relative contribution of each of the cylindrical shells of radius r to the overall response, defined as^[11]:

$$G(r) = \int_0^R \int_{-\infty}^{\infty} g_{Doll}(\rho, z) dz d\rho \quad (2)$$

Different array induction tools have different structure parameters (see in Fig.1) and geometry factors, but same depth of investigation appeared after software synthetic focusing. Fig.2(A) shows the relationship of the radial geometry factors of seven sub-arrays in HDIL tools and the invaded depth, and Fig.2(B) is the radial geometry factor of different depths of investigation after software synthetic focusing, the software is designed by the author, RTOPT.

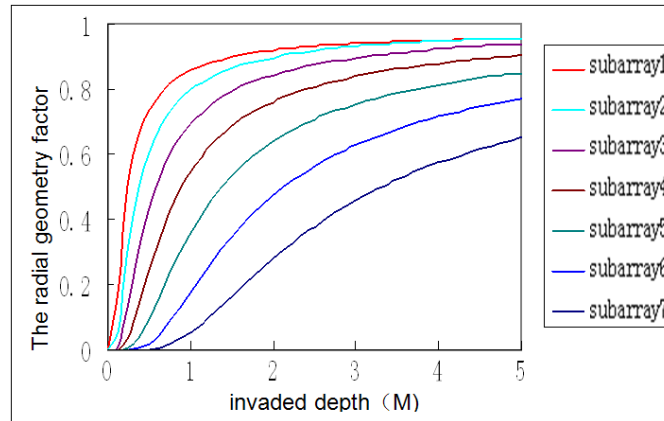


Fig.2(A) The radial geometry factor vs. invaded depth in HDIL tools

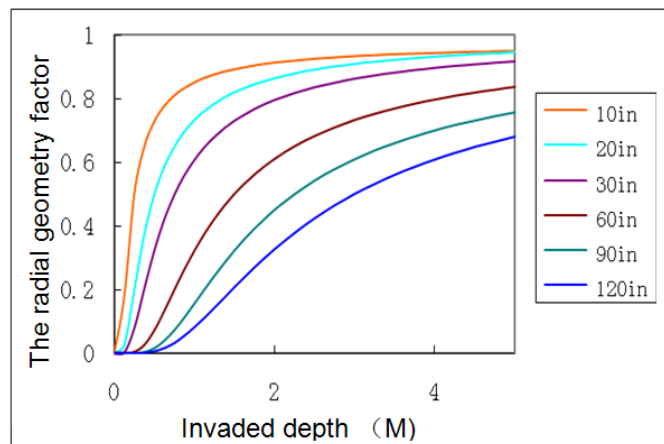


Fig.2(B) The radial geometry factor of six depths of investigation

III. FORMATION RESISTIVITY MODELS

In the inversion procedure of array induction logging, the formation resistivity model is crucial to the reality and precision of inversion results. The most common models are the linear invaded model, three-step invaded model and reciprocal model^[9-10] of the transitional zone. The linear invaded model can be merged to the exponential model, and the result of reciprocal model is much more identical to the invasion procedure^[11-12]. The parabolic-invaded model has been proposed in recent years. In order to analyze and optimize the inversion model, these four models will be analyzed and compared as follows.

3.1 Exponent-invaded model

Exponent-invaded model's resistivity in invaded zone appears to be an exponential one (see in Eqs.(3), where n varies from 0 to 3, and it is unreasonable when n is too large. Fig.3(A) shows the linear invasion of the resistivity in transition zone (i.e. $n=1$ in Eqs.(3)). In contrast, Fig.3(B) shows the non-linear invasion.

$$C = C_{xo} + (C_t - C_{xo}) \left(\frac{r - D_{xo}}{D_I - D_{xo}} \right)^n \quad (3)$$

Where C , C_{xo} , C_I and C_t represent formation conductivity, flushed zone conductivity, invaded zone conductivity and undisturbed formation resistivity respectively, r is different depths away from the borehole, D_I and D_{xo} are the depths of flushed zone and invaded zone.

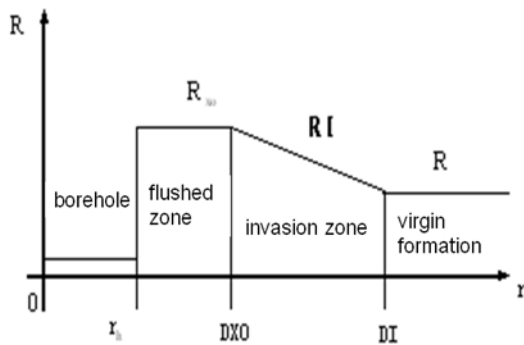


Fig.3(A) Linear-invaded model

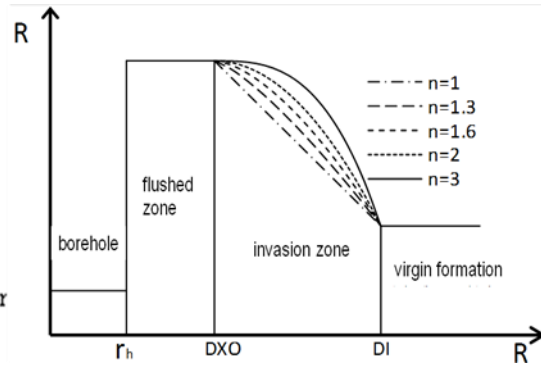


Fig.3(B) Exponent-invaded model

3.2 Reciprocal-invaded model

Reciprocal-invaded model is also a ordinary inversion model as illustrated in Fig.3(C), and it is adopted by Baker Atlas, which is

$$C = C_t + \frac{(C_{xo} - C_t)}{1 + (L / Li)^n} \tag{4}$$

Where, Li is the mean value of invasion radius, n is the index of transitional zone, and L is the invasion depth. The key point in this model is to obtain n through the inner and outer radius $Li1$, $Li2$ of the transition zone: $Li1 = Li \cdot (1 - (2/n))$, $Li2 = Li \cdot (1 + (2/n))$.

The computed n is a constant due to the defined value of inner and outer radius $Li1$, $Li2$. However, the model becomes discontinuous as shown in Fig.3 (D), in controversy with the real situation. Therefore, we modify this model to assign n a variant, of which the variation value is ranged from 10 to 20 or -20 to -10, as a result, sound continuity of formation resistivity is achieved (the positive value represents the resistivity from high to low, the negative one represents the resistivity from low to high)

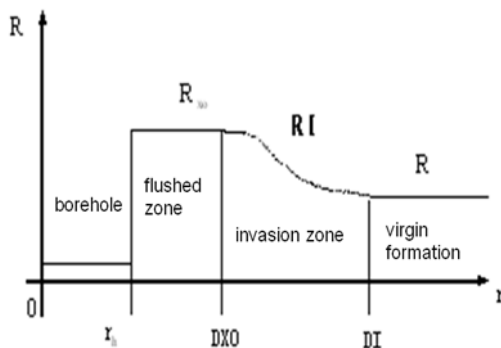


FIG.3(C) Reciprocal-invaded model

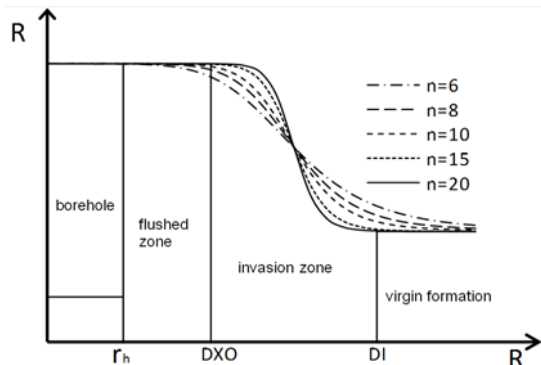


FIG.3(D) Continuity of the resistivity vs. n

3.3 Step-invaded model

Step-invaded model treats the three resistivity values as mean value of flushed zone, transitional zone and undisturbed zone respectively (Fig.3 (E)), which is suitable for the high or low invasion in common and reflects the low or high resistivity zone, thus extensively applied in the inversion. The defect is that it cannot reflect the real formation resistivity variation.

3.4 Parabolic-invaded model

In oilfield, mud invasion is complex, for example, transitional zone resistivity may less than those in invasion zone and flushed zone, so both the exponent-invaded model and reciprocal-invaded model are not suitable for inversion. Therefore, the parabolic-invaded model is properly introduced as in Fig.3 (F). The parabolic-invaded formula which is proposed by the author expressed as:

$$C = a(r - L_m)^2 + R_{im} \tag{5}$$

Where, R_{im} is the extreme value of the parabolic, a is the quadratic coefficient of the model, and L_m is the depth of extreme resistivity.

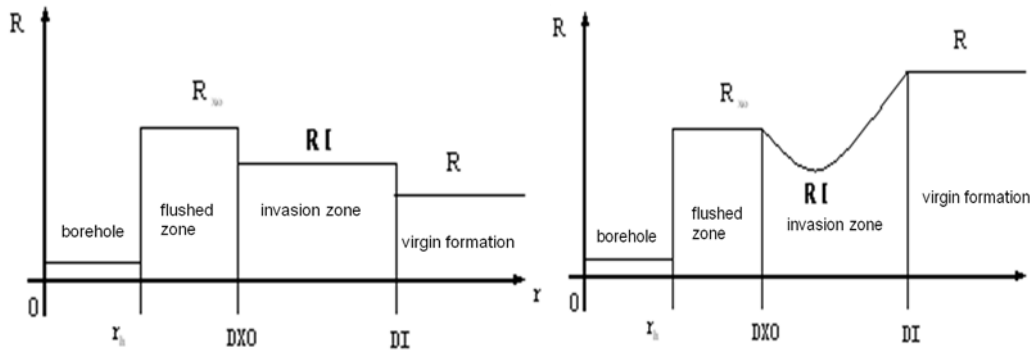


Fig.3(E) Step-invaded model

Fig.3(F) Parabolic-invaded model

IV. NUMERICAL SIMULATION OF ARRAY INDUCTION

The inherent geometry factor^[11-12] and radial resistivity model can be used to build up the response equations of array induction logging.

4.1 Construction of the response equations

Initially, the step-invaded model is considered firstly. The measured conductivity is the multiply of three conductivity values and their geometric factors, as author's Eqs.6:

$$C_a = G_{xo} * C_{xo} + (G_I - G_{xo}) * C_I + (1 - G_I) * C_t \quad (6)$$

Where, Ca, Cxo, CI and Ct represent conductivity, flushed zone conductivity, invaded zone conductivity and formation conductivity respectively. G_I and G_{xo} are the lateral geometric factors of invaded zone and flushed zone respectively.

Similarly, the response equation of other models is obtained, according to author's research:

$$C_a = G_{xo} * C_{xo} + \int_{D_{xo}}^{D_I} G(r) C_I dr / (D_I - D_{xo}) + (1 - G_I) * C_t \quad (7)$$

Where, G(r) is radial geometric factor curve, and CI indicates invasion zone conductivity in exponent-invaded model, reciprocal-invaded model and parabolic-invaded model.

The resistivity of invaded zone is constant in Eqs.6, which can be merged into Eqs.7, as a result, the author gives an universal response equation:

$$C_{ij}(a) = G_{ij}(xo) * C_{xo} + \int_{D_{xo}}^{D_I} G_{ij}(r) C_I dr / (D_I - D_{xo}) + (1 - G_{ij}(I)) * C_t \quad (8)$$

Where, the subscript i means the ith depth of investigation of the response and the subscript j is the radial geometry factor of the jth depth of investigation.

4.2 Forward computation

Based on the forward computation of formation models according to the array induction response correlation, assuming the minimum invasion depth is 0.5m and the maximum is 1m, the first model shows a lower invasion while the second model displays a higher one. The index n is 2 and 12 in exponent-invaded model and reciprocal-invaded model respectively. The results are showed in Fig.4, the step-invaded model (A), the exponent-invaded model (B) and the reciprocal-invaded model(C).

The parabolic-invaded model is suitable for the low or high resistivity annulus zones, so two models are built up. The minimum mud invasion depth is 0.5m and the highest depth is 1m. The first model shows the low resistivity zone, and the second one displays the high resistivity zone. The results are shown in Fig.4 (D).

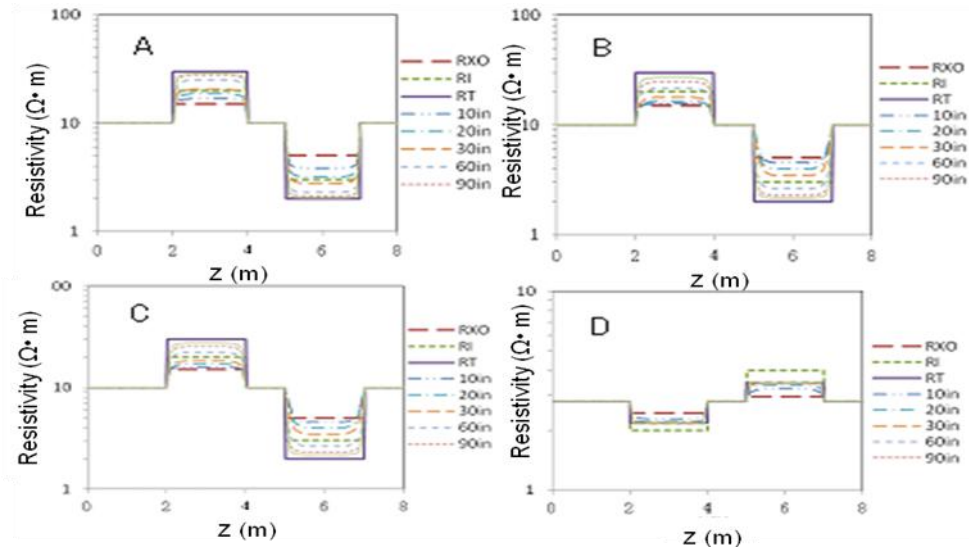


Fig.4 Forward computation of four models

V. INVERSION ALGORITHM

5.1 Construction of inversion objective function

The optimal inversion in array induction is on the basis of generalized inversion in geophysics, which compares practical logging values with theoretic logging values from the interpretation model and the response equation by selecting proper initial values of the parameters in the models. When the enough approximation is satisfied, the unknown parameters represent the parameters in real formation adequately. The objective function is based on the principle of non-linear weighted least square and the theory of error which is written as

$$\min F(x, a) = \min \sum_{i=1}^m \frac{[a_i - f_i(x, z)]^2}{\sigma_i^2 + \tau_i^2} + \sum_{j=1}^p \frac{g_j^2(x)}{\tau_j} \quad [29,30] \quad (9)$$

Where, a_i is the logging values after environmental correlation, x is inversion variant, z is logging depth, $f_i(x, z)$ is the response equation for the i th depth of investigation, σ_i is the error of the i th practical logging value, τ_i is the error of the i th response value, $F(x, a)$ is the optimal objective function, $g_j(x)$ and τ_j is the j th inequality constraint and the error of x .

The errors in Eqs.9 are important to the inversion results^[26-29]. The measurement error is the sum of errors from well diameter, zero drift of the conductivity, the low resolution along the hole, and the correlations etc.

$$\sigma_i^2 = \sum_{k=1}^6 \sigma_k^2 \quad (10)$$

Where, the subscript k is the k th error.

The response error is computed by the author as

$$\tau_i = 0.01 * G_{xo}^2 * C_{xo}^2 + 0.01 * (G_I - G_{xo})^2 * C_t^2 + 0.01 * (1 - G_I)^2 * C_t^2 \quad (11)$$

5.2 Optimal inversion algorithm selection

The optimal algorithm is first compatibly used in logging interpretation and polymineral inversion by Schlumberger, Halliburton and Western-Atlas, which combined one and multi-dimension searching. One dimension searching can be implemented by Golden Section Method, Fibonacci Method, Advance and Retreat Method, Aitken Interpolation Method, PIA. Multi-dimension searching can be finished by DFP(a method proposed by Davidon, Fletcher, Powell) or BFGS Variable Metric Method, Gauss-Newton Least Squares Method, Conjugate Gradient Method and Most Rapid Decline Method^[13]. The GLOBAL in Schlumberger and the ULTRA in Halliburton adopt the Most Rapid Decline Method, whereas the OPTIMA in Western-Atlas embraces the Conjugate Gradient Method^[15-17]. Yong S. H. and Sun J. M. use the combination of the two searching to inverse the data, and have studied the computing times, iteration times, occupation time of the computer, requirements to the initial point and the minimum of the objective function^[13, 29-30]. Even though these methods have some available benefits, there are also some disadvantages, for example, multi-dimension searching may bring negative errors for variational function such as array introduction geometry factor; Conjugate Gradient Method can improve converge accuracy in only first order convergence; Most Rapid

Decline Method may appear serration in curves which impact convergence rapid.

By contrast, the optimal method in this paper can adapt to objective function effectively, increasing searching rapid. The optimum solution in Eqs.9 is a inequality constrained optimization problem, adding a penalty function to the objective function, leading the constrained optimization problem into a series of unconstrained optimization problems. Inversion algorithm is selected by the analysis of the characteristics of the objective function combined with the merits and demerits of the algorithm itself. The objective function is a secondary parabolic equation, in the choice of parabolic interpolation algorithm (PIA) in the one-dimensional search algorithm, which can effectively adapt with objective function and increase the search speed.

Gauss-Newton least square method in multi-dimensional searching is to linear the objective , where the iterative process using linear least squares solution to approximate the nonlinear least-squares solution, so the various array induction differential geometry factor will produce large errors. The steepest descent method uses the fastest decline in the direction of the objective function to determine the direction of the next iteration the process of optimization iteration, i.e. the negative gradient direction. Thus, the convergence speed is not as well as quadratic convergence, while steepest descent algorithm often produces aliasing which affects the convergence rate. The conjugate gradient method uses the negative gradient direction of the initial point as the initial conjugate vector, and the next conjugated direction is determined from the linear combination of negative gradient direction of the previous iteration point and the retrieved conjugated vectors. This algorithm overcomes saw tooth phenomenon, besides, its iterative formula is relatively simple, doesn't need to calculate a second-order derivative of the objective function, reducing the amount of computation and storage, which can improve convergence speed, but still a first-order convergence. BFGS method and DFP method use the quadratic convergence which is fast convergence. The DFP algorithm can be deemed as a specific BFGS method, while the correction matrix in BFGS is not readily to be transferred to a singular matrix, but can reach the global convergence. Thus, the inversion process selects BFGS variable metric method for multidimensional search.

In this paper, the inversion algorithm chooses the BFGS variable metric method and PIA. The one-dimensional searching algorithm is to calculate the best step of inversion variable change process and to determine the minimum point of the parabola; BFGS variable metric method can quickly determine multiple inversion variable search direction. The actual calculation results show that the computing speed of the algorithm in the inversion of array induction is quite rapid, and is able to deal in the sandstone and mudstone strata continuously.

5.3 Inversion quality evaluation

Confidence Interval Method, Fitting Coefficient Method, Optimization of the Objective Function and Reduction of the Non-Correlation Function are usually used to determine the inversion quality^[13]. The confidence interval method and the objective function optimization are adopted in this paper. If the curve is within the confidence interval controlled by the curve of measurement errors, the inversion results are hence reliable; The optimization of the objective function is the total symbol of measuring the theoretical logging curve approximation of the actual logging curve, and the value $F(x, a)$ can be used as a relative quality indication of the calculation results, a smaller result means a better inversion results. Evaluation methods can be seen in the next section.

VI. RESULTS ANALYSIS

6.1 Inversion results comparison of four models

The same array induction materials are used to be applied by using the step-invaded model, the exponent-invaded model, and the reciprocal-invaded model, the results are shown in Fig.5 (A), Fig.5 (B), and Fig.5(C) respectively. The curves from the first track to the forth track represent array induction logging, constructed curves, three-resistivity, and invasion depth separately. From Fig.5 (A), Fig.5 (B), and Fig.5(C), it can be observed that the constructed curves have the same values of C_{X0} , C_T , D_{X0} and D_I . The index n in Fig.5 (B) varies from 0 to 3 and in Fig.5(C) varies from -20 to -15.

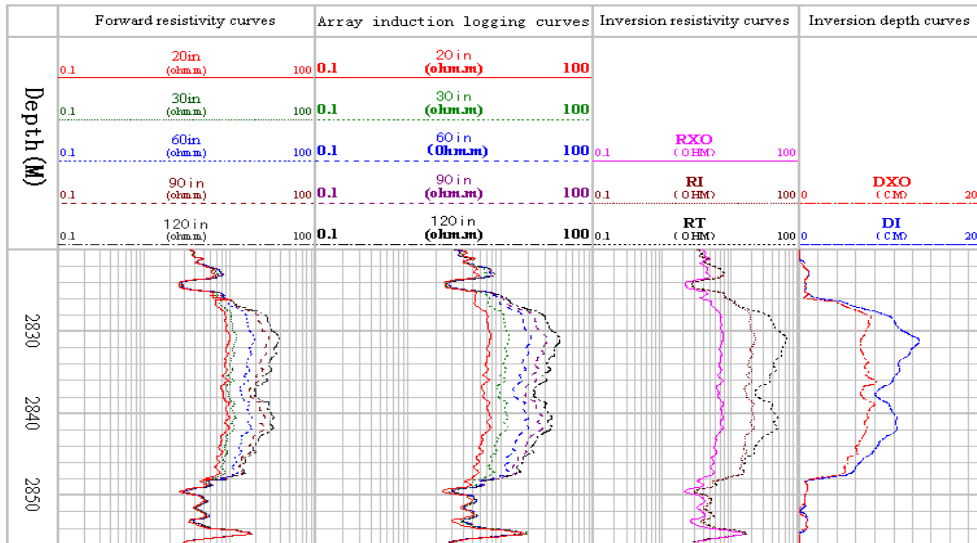


Fig.5(A) Inversion results of the step-invaded model

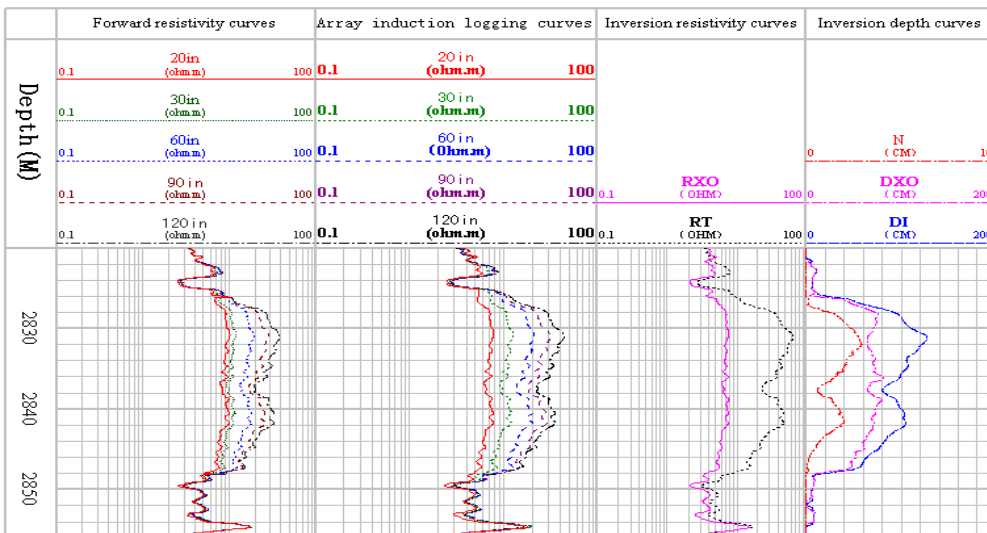


Fig.5(B) Inversion results of the exponent-invaded model

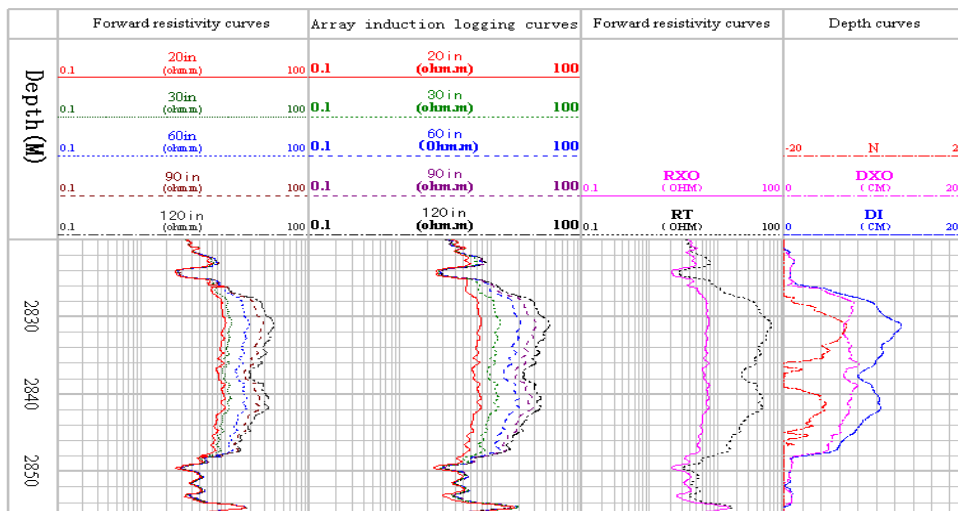


Fig.5(C) Inversion results of the reciprocal-invaded model

Only the parabolic-invaded and the step-invaded model can be applied in the low or high resistivity annulus zones. Fig.5 (D) shows inversion results of a low resistivity annulus zone in a certain well. The inversion resistivity curves of the two models in flushed zone and undisturbed zone is identical, nevertheless, the invaded minimum resistivity of the parabolic-invaded model is much less than that of the step-invaded model, the depth on the transition extreme resistivity of the parabolic-invaded model is in between of the two invaded depth of the step-invaded model. The quadratic coefficient a varies from 0.1 to 0.8.

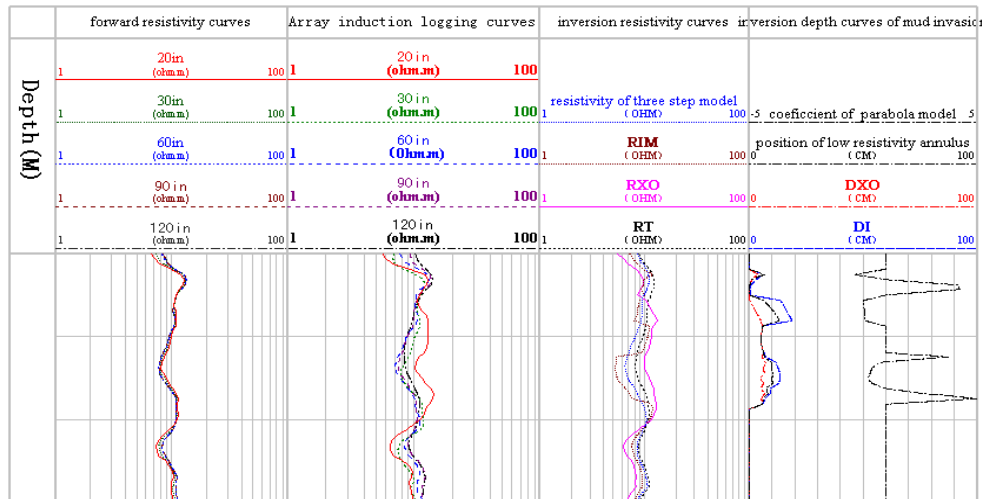


Fig.5(D) Inversion results of the parabolic-invaded model

The inversion algorithm used in the four models gives identical results which demonstrate that it is reliable and efficient. In the general case, the reciprocal-invaded, step-invaded and the parabolic-invaded model can give better inversion results than the exponent-invaded model; in the case that exists the low or high resistivity annulus zone, the step-invaded and parabolic-invaded model can give better results whereas the other two cannot obtain reasonable interpretation of the inversion results.

6.2 Three inversion examples

6.2.1 Formation resistivity profile inversion

Fig.6 includes measured curve, confident interval and constructed curve in the second to sixth track, and the eighth track shows the formation resistivity profile. The confident interval shows a narrow range, implying that the errors in logging curves are small and the stability is high. In addition, the constructed curve fits well to the measured one and the data are within the confident interval.

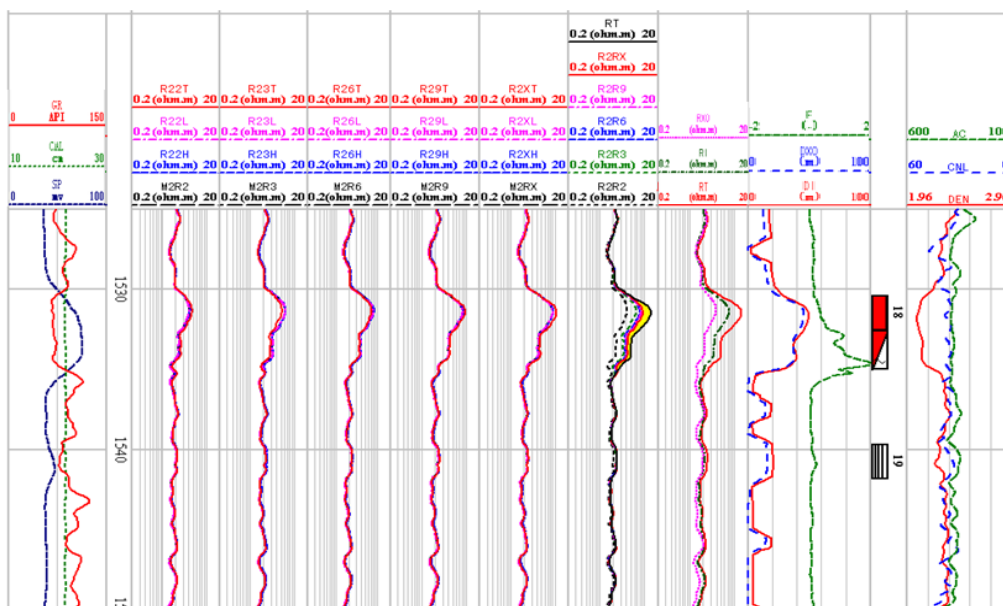


Fig.6 Interpretation of the array induction inversion

6.2.2 Invaded depth inversion

In Fig.7, a relative serious diameter extension of borehole leads to a lower quality of measured curve and a wider range of confidence intervals. The larger objective function calculated in the inversion process displays that the inversion results are affected by borehole diameter extension. A good consistency of the constructed and measured curve indicates that the inversion results of two invasive depths and three-resistivity curve values are reasonable. Moreover, the obvious separation of array induction resistivity curves shows that the resistivity in flushed zone is low and which is high in real formation; in addition, the mud invasion is deep, while the flushed zone depth is relatively small with a large variation.

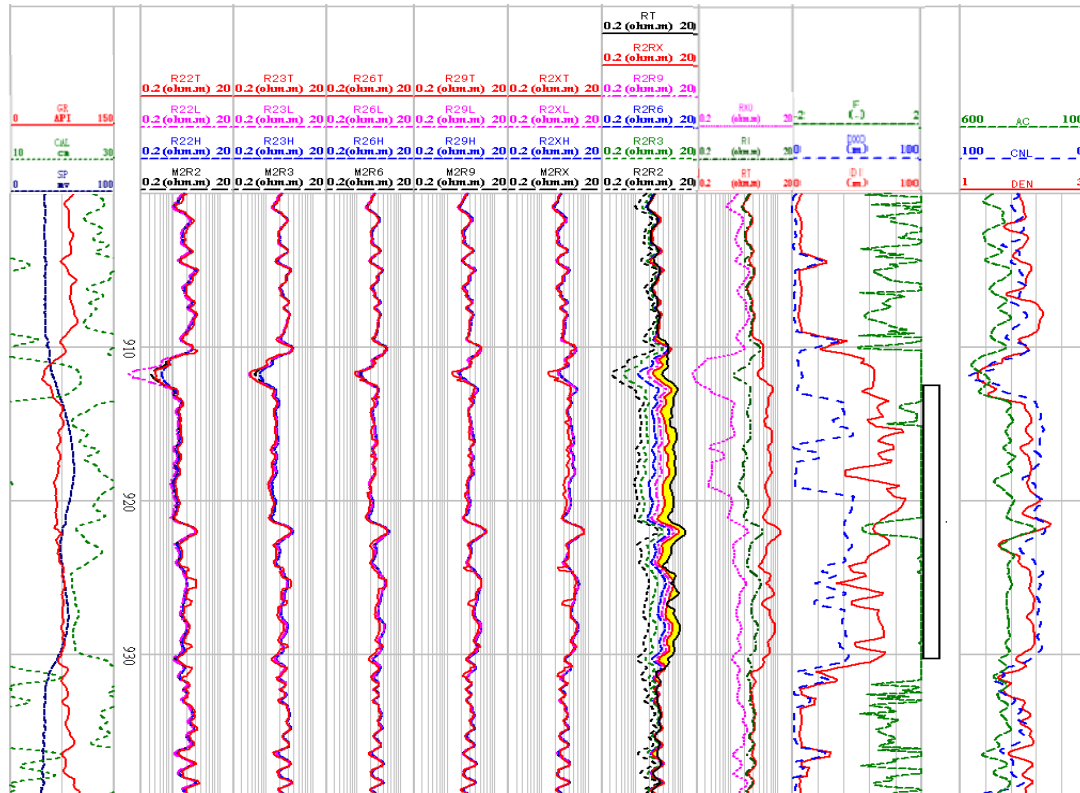


Fig.7 Interpretation of the array induction inversion

6.2.3 Distinguishing the low resistivity annulus zone

In Fig.8, a good consistency of the constructed within the confident intervals and the measured curve indicates that the inversion results of the two invasive depths and three-resistivity curve values are reasonable, which is using a software developed by the author, RTOPT. The inversion results show that the invasion depth is shallow, which may indicate a low atmosphere and low permeability formation. The resistivity of transitional zone is lower than that of the undisturbed zone in the third layer indicates a low resistivity annulus zone, which is interpreted as the oil-water layer and has been verified by oil test.

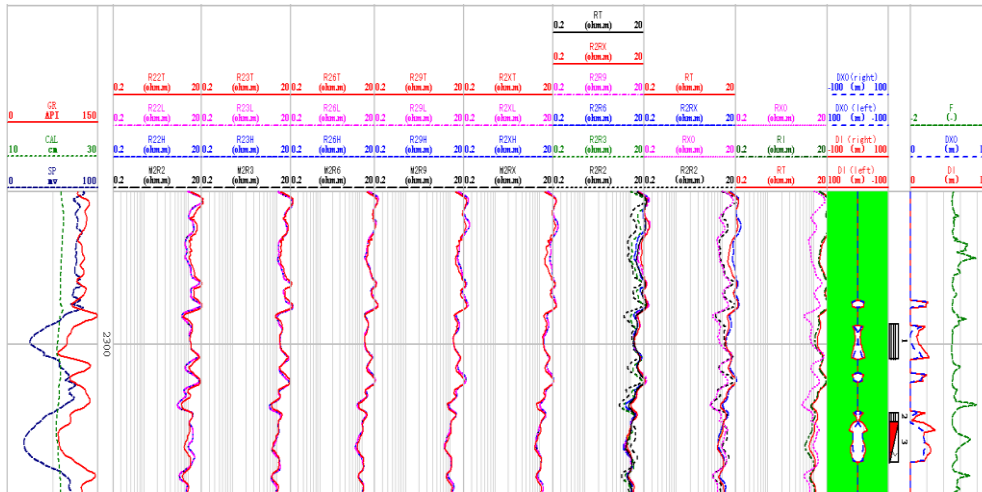


Fig.8 Interpretation of the array induction inversion

VII. DISCUSSION AND CONCLUSION

7.1 Discussion

The inversion algorithm in this paper is an approximate one, but the broad inversion method takes no consideration of the effects of surrounding rocks. When the reservoir is greater than 10in in thickness, this inversion will get good results, rather the contrary. The surrounding rock correction need to be performed first before inversion in thin reservoir.

In parabolic-invaded model(Eqs.5), there are the resistivity extreme points in transition zone which are not the case when only low or high inversion in the practical formation. Hence, this model can only be used when the low or high resistivity annulus zones exist.

When the curves of array induction are essentially coincident, the invasion depth is not sensitive to the raw logging curves according to the Eqs.6 to Eqs.8, and the inversion results rely on the initial value of the invaded depth, thus, a initial value must be chosen carefully before the inversion. Fortunately, when the curves are not completely superposition and the range of the initial points is wide enough, there has little effect on array induction logging.

The quality of inversion also lies on the measured data. If the data quality is poor, unsatisfied results can be obtained in spite of introducing the errors. As a result, the environmental correlation is necessary before the inversion, and the size of borehole has an important influence on inversion data, even reduce the credibility of inversion. Thus, the method to correlate the effect of borehole based on the geometry factor, which proposed by author:

$$C'_a = \frac{C_a - G(r)C_m}{1 - G(r)} \quad (12)$$

Where, C_m , C_a , C'_a and $G(r)$ are conductivity of the mud, measured conductivity of the formation, correlated conductivity the radial geometry factor.

7.2 Conclusion

Through constructing the response equation of the array induction logs, optimizing the inversion algorithm and inverting three examples, five conclusions are achieved as follows:

- Different tools, which have different constructions of coil system and geometry factors have a same investigation depth. after a software focusing, thus it is suitable to use geometry factors to build up the response equations for all array induction tools;
- Step-invaded model has a general applicability while the exponent-invaded and the reciprocal-invaded model can be applied to a high or low invaded formation. The parabolic-invaded model functions can be applied only when low or high resistivity annulus zone exists;
- The present reciprocal-invaded model is modified to reduce the errors in the model;
- The inversion algorithm combined with BFGS and PIA method is stable and fast, possibly to continuous processing;
- The results of undisturbed zone resistivity and the invasion profiles are positive to the numerical correlation of the resistivity largely affected by the high and deep invasion.

ACKNOWLEDGEMENTS

This work is supported by National Natural Science Foundation of China (Grant No.41074102 and 41130417), “111 Program” (B13010) , Program for Changjiang Scholars and Innovative Research Team in University.

- [1] Lin Y, Gianzero S, Strik land R. Inversion of Induction Logging Data U sing Least Square Technique. SPWLA 25th Annual Logging Symposium, June 1984.
- [2] Chew W C and Liu Q H. Inversion of Induction Tool Measurements Using the Distorted Born Iterative Method and CG-FFHT. IEEE, GE32, 1994 (4).
- [3] Zhang Z Q, Zhang G J, et al. Reconstructing Two dimensional Resistivity Profile Using Array Induction Logs [J]. Well Logging Technology, 1997, 21(2).
- [4] Zhang Z Q, Zhang G J, et al. Multi parameters Inversion of Formation Resistivity Profile Using Array Induction Log [J]. Well Logging Technology , 1998, 22(5).
- [5] Zhang Y R and Nie Z P. A Nonlinear Inversion Approach to Formation Conductivity——Inversion of AIT Measurements [J]. Well Logging Technology , 1997, 21(5).
- [6] Wei B J. Computation Of Array Induction Logging Response Using Integral Equations [J]. Journal of China University of Petroleum(Edition of Natural Science) , 2005, 29(6).
- [7] Liu J Q and Kuang Z. The Iteration Method For Solving Formation Resistivity [J]. Chinese Journal Geophysics, 1998,32(Supplement)
- [8] Zhao M, Gao J, et al. Joint Inversion Study of Conventional Electrical Logging and Its Applications [J]. Well Logging Technology , 2003, 27(1).
- [9] Liu Z H, Wu J, et al. Sequent Inversion For The Logging Data Of Array Induction tool[J]. Progress in Geophysics, 2006, 21(4).
- [10] Zhang Y R and Nie Z P. Inversion Of The Formation Conductivity Using The Measurements Of Array Induction Imager Tool [J]. Chinese Journal Geophysics, 1998, 41(4).
- [11] Zhang G J. Electrical Logging [M]. Beijing: Petroleum Industry Press, 2009.
- [12] Zhang J H, Liu Z H, et al. The Principle and Application of Electrical Logging [M]. Xi'an: Northwest University Press, 2002.
- [13] Yong S H. Optimum Logging Interpretation [M]. Dongying: University Of Petroleum Press, 1995.
- [14] Li Q Y, Wang N C, et al. Numerical Analysis [M]. Huazhong University of Science and Technology Press, 1982.
- [15] Mayer C. and Sibbit A. GLOBAL-A New Approach to Computer Precessed Log Interpretation, SPE 9341, 1980.
- [16] Albery M. and Hashmy K. H., Application of ULTRA to Log Analysis, SPWLA 25th Annual Logging Symposium, June, 1984.
- [17] Mezztes A., Rodrigue E. & Frost E., OPTIMA-A Statiscat Approach to Well Log Analysis, International Symposium Petroleum Exploration in Carbonate Areas, Nanjing, China, November 12-19, 1986.
- [18] Gysen M., Mayer C. and Hashmy K. H., A New Approach to Log Analysis Inversing Simultaneous Optimization of Unknown and Zoned Parameters, 11th Formation Evaluation Symposium, 1987.
- [19] Hashmy K.H. and Albery M.W., Use of Physical Samples and Inverse Log Evaluation for Improved Formation Analysis, 1986.
- [20] Dresser Atlas. A Statistical Approach to Well Log Analysis, 1986.
- [21] Howard A Q. A new invasion model for resistivity log interpretation. The Log Analyst, March-April, 1992.
- [22] Singer J and Barber T. The effect of transition zones on the response of induction logs. Presented at the 28th annual SWPLA logging Symposium, 1998.
- [23] Ehon Head, Darrel Cannon, David Allen, Leif Colson. Quantitative invasion description. SPWAL 33rd annual logging symposium. June 1992, B1.
- [24] Xiao L Z. An Improved Method Of Optimum Interpretation Of Well Logs. Acta Petrolei Sinica, 1991, Vol.12(2).
- [25] Xiao L Z. Study On The Incoherence Function In Global Program, Acta Petrolei Sinica, 1990, Vol.11(2).
- [26] Xiao L Z. Theory For The Optimum Interpretation Of Well Logging, Geophysical Prospecting For Petrole, 1988, Vol.27(2).
- [27] Xiao L Z. Evaluation For The Result Obtained From Optimal Well Logging Interpretation, Geophysical Prospecting For Petrole, 1989, Vol.28(2).
- [28] Xiao L Z. Effect of Quality Control in Optimum Log Interpretation Technique, Borehole Geophysics, 1989, Vol.13(2).
- [29] Yong S H, Sun J M, et al. Evaluation of Complex Reservoirs Using Optimization Method [J]. Well Logging Technology , 1988, 12(4).
- [30] Yong S H and Sun J M. Selection Of The Optimization Method For Digital Well Logging Data Processing, Journal of China University of Petroleum (Edition of Natural Science), 1988.
- [31] Chang W H, Pan H P, et al. Two-Dimensional Numerical Simulation of Mud Invasion [J]. Earth Science (Journal of China University of Geosciences), 2010, 35(4).
- [32] Ma M X and Ju B S. A Novel Mathematical Model to Calculate Distribution of Mud Invasion Formation Resistivity [J]. Well Logging Technology , 2004, 28(6).

Dongliang Liao. "Optimal Inversion of Array Induction Log." *International Journal of Engineering Science Invention (IJESI)*, Vol. 09(10), 2020, PP 49-60. Journal DOI- 10.35629/6734